

ORIGINAL RESEARCH

Laminin-221 Enhances Therapeutic Effects of Human-Induced Pluripotent Stem Cell-Derived 3-Dimensional Engineered Cardiac Tissue Transplantation in a Rat Ischemic Cardiomyopathy Model

Takaaki Samura , MD; Shigeru Miyagawa, MD, PhD; Takuji Kawamura, MD, PhD; Satsuki Fukushima, MD, PhD; Jun-ya Yokoyama, MD; Maki Takeda, PhD; Akima Harada, BSHS; Fumiya Ohashi, PhD; Ryoko Sato-Nishiuchi, PhD; Toshihiko Toyofuku, PhD; Koichi Toda, MD, PhD; Kiyotoshi Sekiguchi, PhD; Yoshiaki Sawa , MD, PhD

BACKGROUND: Extracellular matrix, especially laminin-221, may play crucial roles in viability and survival of human-induced pluripotent stem cell-derived cardiomyocytes (hiPS-CMs) after in vivo transplant. Then, we hypothesized laminin-221 may have an adjuvant effect on therapeutic efficacy by enhancing cell viability and survival after transplantation of 3-dimensional engineered cardiac tissue (ECT) to a rat model of myocardial infarction.

METHODS AND RESULTS: In vitro study indicates the impacts of laminin-221 on hiPS-CMs were analyzed on the basis of mechanical function, mitochondrial function, and tolerance to hypoxia. We constructed 3-dimensional ECT containing hiPS-CMs and fibrin gel conjugated with laminin-221. Heart function and in vivo behavior were assessed after engraftment of 3-dimensional ECT (laminin-conjugated ECT, n=10; ECT, n=10; control, n=10) in a rat model of myocardial infarction. In vitro assessment indicated that laminin-221 improves systolic velocity, diastolic velocity, and maximum capacity of oxidative metabolism of hiPS-CMs. Cell viability and lactate dehydrogenase production revealed that laminin-221 improved tolerance to hypoxia. Furthermore, analysis of mRNA expression revealed that antiapoptotic genes were upregulated in the laminin group under hypoxic conditions. Left ventricular ejection fraction of the laminin-conjugated ECT group was significantly better than that of other groups 4 weeks after transplantation. Laminin-conjugated ECT transplantation was associated with significant improvements in expression levels of rat vascular endothelial growth factor. In early assessments, cell survival was also improved in laminin-conjugated ECTs compared with ECT transplantation without laminin-221.

CONCLUSIONS: In vitro laminin-221 enhanced mechanical and metabolic function of hiPS-CMs and improved the therapeutic impact of 3-dimensional ECT in a rat ischemic cardiomyopathy model. These findings suggest that adjuvant laminin-221 may provide a clinical benefit to hiPS-CM constructs.

Key Words: 3-dimensional engineered cardiac tissue ■ heart failure ■ human-induced pluripotent stem cells ■ laminin-221 ■ regenerative therapy

Although cardiac transplantation and left ventricular (LV) assist device implantation are the standard-of-care treatment for end-stage heart failure, donor shortages and critical complications of LV assist device severely limit these interventions.¹⁻³ For these reasons, regenerative therapy may provide

Correspondence to: Yoshiaki Sawa, MD, PhD, Department of Cardiovascular Surgery, Osaka University Graduate School of Medicine, Yamadaoka 2-2, Suita City, Osaka 565-0871, Japan. E-mail: sawa-p@surg1.med.osaka-u.ac.jp

Supplementary Materials for this article are available at <https://www.ahajournals.org/doi/suppl/10.1161/JAHA.119.015841>

For Sources of Funding and Disclosures, see page 14.

© 2020 The Authors. Published on behalf of the American Heart Association, Inc., by Wiley. This is an open access article under the terms of the Creative Commons Attribution-NonCommercial License, which permits use, distribution and reproduction in any medium, provided the original work is properly cited and is not used for commercial purposes.

JAHA is available at: www.ahajournals.org/journal/jaha

CLINICAL PERSPECTIVE

What Is New?

- Enhancement of viability and survival of transplanted human-induced pluripotent stem cell-derived cardiomyocytes (hiPS-CMs) may improve the clinical effectiveness of hiPS-CM therapy for heart failure.
- Extracellular matrix, especially laminin-221, may play crucial roles in viability and survival of hiPS-CMs.
- This indicates that laminin-221 enhances therapeutic efficacy by improving cell viability and survival after transplantation of 3-dimensional engineered cardiac tissues to a rat model of myocardial infarction.

What Are the Clinical Implications?

- Laminin-221 enhanced mechanical and metabolic function of hiPS-CMs and demonstrated improved therapeutic potential of 3-dimensional engineered cardiac tissue in a rat ischemic cardiomyopathy model.
- These findings suggest that adjuvant laminin-221 may enhance clinical effect of hiPS-CM therapy to patients with heart failure.

Nonstandard Abbreviations and Acronyms

ECM	extracellular matrix
hiPS-CMs	human-induced pluripotent stem cell-derived cardiomyocytes
LDH	lactate dehydrogenase
L-ECT	laminin-conjugated engineered cardiac tissue
3D-ECT	3-dimensional engineered cardiac tissue

an alternative approach to restore impaired heart function.

Despite the potential of regenerative therapies, recent studies have found that human-induced pluripotent stem cell-derived cardiomyocytes (hiPS-CM) implantation via cell sheet, engineered cardiac tissue (ECT), and needle injection in animal heart models results in low engraftment rate and limited therapeutic success in severe heart failure.^{4,5} The keys to prolonging hiPS-CM survival are blood supply to transplanted tissue, reduction of immunogenicity after transplant, and an appropriate niche that enhances cardiomyocyte viability.⁶ Previous work to improve hiPS-CM survival through the blood supply has found that cell sheet implantation combined

with omentum-induced mature vasculature in both the transplanted sheet and the recipient heart leads to better cell survival.⁷ Immunogenicity from the innate immune response can be significantly reduced by major histocompatibility complex matching, and the suppression of natural killer cells leads to prolongation of cell survival. As for extracellular matrix (ECM), laminin, especially laminin-221, is a major component known to have the best affinity to cardiomyocytes, and plays an important role to avoid anoikis of transplanted cardiomyocytes via integrin signals.⁸⁻¹⁰

Therefore, we hypothesized that adjuvant laminin-221 improves the therapeutic efficacy of 3-dimensional ECT (3D-ECT) transplantation in a rat model of myocardial infarction (MI) by enhancing cell viability and survival.

METHODS

The data that support the findings of this study are available from the corresponding author on reasonable request.

hiPS-CM Culture and Differentiation to Cardiomyocytes

hiPS-CMs (253G1; Riken, Ibaraki, Japan) were cultured and maintained in Primate ES Cell medium (ReproCELL, Kanagawa, Japan) with 4 ng/mL human basic fibroblast growth factor (Wako, Osaka, Japan) on mouse embryonic fibroblast cells (ReproCELL). Cardiac differentiation was induced using the bioreactor system, as previously described.¹¹⁻¹³ Briefly, hiPS-CMs were dissociated using a dissociation solution (ReproCELL) and transferred to an ultralow attachment culture dish (Corning, MA) in mTeSR1 (Stemcell Technologies, Canada) with Y-27632 (Wako). After the formation of embryoid bodies, the culture medium was exchanged for a differentiation medium that contained StemPro34 (Thermo Fisher Scientific, MA), 2 mmol/L L-glutamine (Thermo Fisher Scientific), 50 mg/mL ascorbic acid (Wako), and 1-thioglycerol (Sigma-Aldrich, St. Louis, MO) and was supplemented with several human recombinant proteins, including BMP4 (bone morphologic protein 4), activin A, basic fibroblast growth factor, and VEGF (vascular endothelial growth factor) (R&D Systems, MN), and small molecules, such as IWR-1 (Wako). hiPS-CMs remained in DMEM (Nacalai Tesque, Kyoto, Japan) containing 10% fetal bovine serum (Sigma-Aldrich). We also used PB/CAG-luc2-IP-induced hiPS-CMs (201B7-luc7) to assess bioluminescence imaging. The hiPS-CM cell line 201B7-luc7 cells, generated from human mononuclear cells, were a gift from Professor Yamanaka (Kyoto University, Kyoto, Japan). The

201B7-luc7 cells were cultured on iMatrix511 (Nippi, Tokyo, Japan)-coated dishes in Stem Fit Ak02N (Ajinomoto, Tokyo, Japan). A previously described technique induced cardiac differentiation.¹⁴

Flow Cytometry Analysis of Cardiomyocyte Purity

Cardiomyocytes derived from hiPS-CMs were dissociated with 0.25% trypsin-EDTA (Thermo Fisher Scientific), fixed with CytoFix fixation buffer (Becton Dickinson, Franklin Lakes, NJ) for 30 minutes at 4°C, permeabilized with Perm/Wash buffer (Becton Dickinson) at room temperature for 10 minutes, and then incubated with mouse anti-troponin T antibody (Santa Cruz Biotechnology, Dallas, TX) for 60 minutes at 4°C. The labeled cells were washed with Perm/Wash buffer before incubation with the secondary antibody at room temperature for 30 minutes and then incubated with anti-mouse Alexa Fluor 488 antibody (Invitrogen, 1:1000) for 30 minutes at 4°C. The samples were assayed using flow cytometry (FACSCanto II; BD Biosciences, CA), and the results were analyzed using BD FACSDiva software (BD Biosciences).

Recombinant Laminin-221

Human laminin-221 produced recombinant and functionally active E8 fragments.^{9,15,16} Recombinant laminins were expressed using a FreeStyle 293 Expression System (Life Technologies, Carlsbad, CA) and purified by sequential affinity chromatography using Ni-NTA-agarose (Qiagen, Carlsbad, CA) and anti-FLAG-M2-agarose (Sigma).

ECT Fabrication

To generate 3D-ECT, we used fibrin gel as a scaffold. Although it was required to use a low concentration of fibrin gel for good survival of hiPS-CM, a low concentration of fibrin gel makes it challenging to form the arbitrary shape and size of 3D-ECT.¹⁷ In the present study, we used a novel simple and pragmatic technique to fabricate 3D-ECT. First, we prepared a polypropylene sheet (cut for 10 × 10 mm from clear folder) and DMEM gelatin-coated 6-well plate (1.6 g gelatin was dissolved in 40 mL DMEM containing 10% fetal bovine serum and was poured into each well, 2.0 mL of DMEM with gelatin). hiPS-CMs (5×10^6 cells in 100 μ L cardiac media [DMEM {Nacalai Tesque, Kyoto, Japan} containing 10% fetal bovine serum]) were mixed with 10 μ L human fibrinogen (Berioplast P Solution A was diluted 2 times by DMEM, 40 μ g/ μ L) and 10 μ L laminin-221 (120 nmol/L) or 10 μ L Dulbecco's PBS(-) (Nacalai Tesque, code 14249-24). The mixture of hiPS-CMs, fibrinogen, and laminin-221 or PBS was dropped on DMEM gelatin

gel, then 5 μ L thrombin (Berioplast P Solution B was diluted 10 times by DMEM, 0.03 U/ μ L) was added to the mixture and covered by polypropylene sheet (10 × 10 mm). The 3D cardiac tissue was solidified at 4°C for 10 minutes, then DMEM gelatin gel was dissolved under the cardiac tissue in an incubator (37 °C for 20 minutes) to retrieve cardiac tissue with polypropylene sheet. ECT with laminin-221 was named laminin-conjugated ECT (L-ECT), whereas ECT without laminin-221 was named ECT.

Immunohistochemistry and Histological Methods

In hiPS-CM analysis, plates were pretreated with laminin-221 for laminin group. Dissociated single cells, ECTs, or harvested hearts were fixed with 4% paraformaldehyde and labeled with primary antibodies, followed by incubation with fluorescence-conjugated secondary antibodies. Hoechst 33342 (Dojindo Molecular Technologies, Kumamoto, Japan) counterstained the nuclei. Images were taken on a confocal microscope (FLUOVIEW FV10i; Olympus, Tokyo, Japan).

Quantitative Real-Time Polymerase Chain Reaction

Total RNA from hiPS-CMs in vitro or cardiac tissue after ECT transplantation in vivo was isolated using the PureLink RNA Mini Kit (Thermo Fisher Scientific) or RNeasy Fibrous Tissue Mini Kit (Qiagen, Hilden, Germany), respectively. RNA was reverse transcribed to cDNA using the SuperScript III reverse transcription kit (Thermo Fisher Scientific). Quantitative real-time polymerase chain reaction was performed using ViiA 7 RealTime PCR System (Thermo Fisher Scientific) with TaqMan (Thermo Fisher Scientific) or SYBR green (Thermo Fisher Scientific) probe. All data were normalized using GAPDH as the control and evaluated using the $2^{-\Delta\Delta Ct}$ method. For the in vitro 2-dimensional study, plates were pretreated with laminin-221 for the laminin group. For the in vitro 3D study, we compared L-ECT with ECT. The antibodies are listed in Table S1.

Western Blot Analysis

Protein from whole cells was extracted using 1% radioimmunoprecipitation assay lysis buffer (catalog No. R0278, Sigma) with standard protease and phosphatase inhibitors (catalog No. P8340, Sigma). SDS-PAGE separated proteins from subcellular fractions and whole cell lysate using Criterion 4%–20% Tris-HCl (10–250 kD) gels (Bio-Rad, Hercules, CA). After transfer to polyvinylidene difluoride membranes, the membranes were washed in tris-buffered

saline buffer containing 0.1% Tween 20, then blocked using blocking-one (Nacalai 03953-66). The primary antibodies were diluted in Can Get Signal Solution 1 (TOYOBO NKB-201) and incubated at 4°C for 18 hours. Primary antibodies against focal adhesion kinase (FAK) (1:1000, catalog No. 13009), phosphorylated FAK (Tyr397) (1:1000, catalog No. 8556), GAPDH (1:1000, catalog No. 2118), pS727–signal transducer and activator of transcription 3 (STAT3; 1:1000, catalog No. 9134), STAT3 (1:1000, catalog No. 12640), and α -tubulin (1:1000, catalog No. 2125) were purchased from Cell Signaling Technology (Danvers, MA). After washing in tris-buffered saline, the membranes were incubated in species and isotype-specific horseradish peroxidase–conjugated secondary antibodies in Can Get Signal Solution 2 (TOYOBO NKB-301). Chemiluminescence (catalog No. 34080, Thermo Fisher) was used to reveal immunoreactive protein bands detected by X-ray film or imaged on a Licor Odyssey FC (Lincoln, NE) for 10 minutes. As for the laminin group, plates had been pretreated with laminin-221 before hiPS-CMs were seeded. The antibodies are listed in Table S2.

Cell Motion Analyses

The contractile property was assessed by a Cell Motion Imaging System (SI8000; SONY, Tokyo, Japan). Videos of the hiPS-CM and 3D-ECT were recorded at a frame rate of 150 frames per second, a resolution of 1024×1024 pixels, and a depth of 8 bits. In 2-dimensional analysis, plates were pretreated with laminin-221 for the laminin group. In 3D-ECT analysis, we made 3D-ECT directly onto a 12-well plate and peel out (polypropylene) sheet.

Mitochondrial Function Assay

The Seahorse XF96 extracellular flux analyzer was used to analyze mitochondrial function. Plates were pretreated with laminin-221 for the laminin group. hiPS-CMs were seeded onto the plates (40 000 cells per XF96 well). The cells were cultured at 37°C for 3 days in the Seahorse plates before analysis. The culture medium was exchanged for a basal medium (XF assay medium supplemented with 25 mmol/L glucose and 1 mmol/L sodium pyruvate) 1 hour before the assay, and for the duration of the measurement of oxygen consumption rate (OCR). Substrates and selective inhibitors were injected during the measurements to achieve final concentrations of 25 mmol/L glucose, 2.5 mmol/L oligomycin, 1 μ mol/L carbonyl cyanide-p-trifluoromethoxyphenylhydrazone, 2.5 μ mol/L rotenone, and 2.5 μ mol/L antimycin A. The basal respiration rate was defined as the average values of OCR measured from time point 1 to 4 (0–21 minutes) during the experiment. ATP production

was defined as the difference in OCR between the basal respiration and the OCR value after 2.5 μ mol/L oligomycin injection. Spare respiratory capacity was defined as the difference in OCR between the basal respiration and the OCR value after 1 μ mol/L carbonyl cyanide-p-trifluoromethoxyphenylhydrazone injection.

Cell Viability Assay

The cell viability was assessed using a Cell Counting Kit-8 (Dojindo). In the laminin group, plates had been pretreated with laminin-221 before hiPS-CMs were seeded. hiPS-CMs (5×10^4 /96 wells) were cultured at 37°C for 1 day. During the second day, the media were changed to fresh media, then incubated under hypoxia (5% O₂, 37°C) for 3 days. Then, 10 mL Cell Counting Kit-8 solution was added to each well for incubation for 2 hours at 37°C. Absorbance was recorded on a microplate reader at a wavelength of 450 nm with a reference wavelength of 630 nm. Cell viability was determined as the percentage of surviving cells compared with control. As for the FAK inhibition experiment, hiPS-CMs were cultured with FAK inhibitor 14 (FAK14; 0, 25, or 50 μ mol/L, catalog No. 3414, Tocris) from the second day under hypoxia for 3 days. Then, cell viability was assessed by the above procedure.

Lactate Dehydrogenase Release Assay

A lactate dehydrogenase (LDH) release assay was performed using an LDH Cytotoxicity Detection Kit (Takara Bio, Shiga, Japan). In the laminin group, plates had been pretreated with laminin-221 before hiPS-CMs were seeded. hiPS-CMs (5×10^4 /96 wells) were cultured at 37°C for 1 day. The second day, the media were changed to fresh media, then incubated under hypoxia (5% O₂, 37°C) for 3 days. The mixture of diaphorase/nicotinamide adenine dinucleotide was added to each well. After incubation in a dark room for 30 minutes at room temperature, the absorbance was recorded on a microplate reader (DS Pharma Biomedical, Osaka, Japan) at a wavelength of 490 nm with a reference wavelength of 600 nm. The LDH release was determined as the percentage of LDH release compared with control. As for the FAK inhibition experiment, hiPS-CMs were cultured with FAK14 (0, 25, or 50 μ mol/L, catalog No. 3414, Tocris) from the second day under hypoxia for 3 days. Then, cell viability was assessed by the procedure mentioned above.

Protein Analysis

ELISA kits were used to measure VEGF (R&D Systems) secreted from the cultured cells or cultured 3D-ECT,

according to the manufacturers' instructions. The experiment used media for hiPS-CMs with laminin-221 coating plates, as well as a medium containing L-ECT or ECT.

The media of the hiPS-CMs on laminin-221 coating plate and the media of the L-ECT or ECT were used in this experiment.

Animal Care

The animal care procedures used in this study complied with the *Guide for the Care and Use of Laboratory Animals* (National Institutes of Health publication No. 85-23, revised 1996). Experimental protocols were approved by the Ethics Review Committee for Animal Experimentation of Osaka University Graduate School of Medicine.

MI and 3D-ECT Transplantation

MI was induced in 8-week-old male athymic nude rats (F344·NJcl - rnu/rnu; CLEA Japan, Tokyo, Japan) by permanently ligating the proximal left anterior descending coronary artery. Surgery was performed at 3% to 4% inhaled isoflurane anesthesia. Two weeks later, L-ECTs, ECTs, or a fibrin gel sheet was implanted onto the infarcted area of the heart and subsequently covered by pericardium (L-ECT group, n=10; ECT group, n=10; control group, n=10). Every week during a 4-week assessment period after treatment, cardiac function was assessed by ultrasonography.

Evaluation of Cardiac Function

Cardiac function was assessed using an echocardiography system with a 12-MHz transducer (Sonos 7500; Philips, Andover, MA) 2 weeks after MI and every week until 4 weeks after treatments. Standard transthoracic echocardiography was performed at 3% inhaled isoflurane anesthesia. The LV end-diastolic and end-systolic diameters were measured, whereas the LV end-diastolic and end-systolic volumes (LVEDV and LVESV, respectively) were calculated from the Teichholz formula. The LV ejection fraction (LVEF) was calculated from the following formula: $LVEF (\%) = 100 \times (LVEDV - LVESV) / LVEDV$.

Bioluminescence Imaging of Rats

Bioluminescence imaging of rats was performed under 3% inhaled isoflurane anesthesia. Bioluminescence imaging used the IVIS Lumina II (PerkinElmer) (L-ECT group, n=6; ECT group, n=6) for imaging. Ten minutes before the measurement of luminescence, 150 mg/kg body weight of Rediject D-luciferin Ultra Bioluminescent Substrate (PerkinElmer) was injected intraperitoneally. We used an integration time of 1 minute, where images

were acquired every 2 minutes until observing a steady decline in signal intensity. All images were analyzed with Living Image Software (PerkinElmer).

In Vivo Imaging for Calcium Activity in Transplanted ECT

To visualize the excitation-conduction properties of transplanted 3D-ECT on the heart inside the living body, we used the whole-heart in vivo optical imaging technique. hiPS-CMs were transduced with gCaMP3 (253G1 GCaMP+; Myoridge, Kyoto, Japan), which is a fluorescent calcium indicator, and 3D-ECT was made from the hiPS-CMs inserted with gCaMP3. Two weeks after MI, the 3D-ECT was transplanted onto the infarct area of the heart and covered by the pericardium. Three weeks after the transplantation, we performed a second thoracotomy and reopened the pericardium to expose the 3D-ECT under 3% to 4% inhaled isoflurane anesthesia. Hearts were labeled with voltage-sensitive dye by slowly injecting 3 mL of 5 μ mol/L aminonaphthylethylenylpyridinium (di-4-ANEPPS) into the perfusion line. Fluorescent emissions of gCaMP3 and di-4-ANEPPS were separated into a 510- to 560-nm emission filter for the gCaMP3 and a >600-nm long-pass emission filter for the di-4-ANEPPS. Images were recorded by microscope system (Olympus: MVX10) with image splitter optics (Hamamatsu Photonics W-VIEW GEMINI) and high sensitivity, high-resolution camera (Zyla4.2). Images were analyzed by Image J and MATLAB R2018b.

Statistical Analysis

Data were expressed as the mean and SD. Statistical significance was determined by Student's *t*-test (2 tailed) for comparisons between 2 groups. When the 1-way repeated-measures ANOVA test was significant, group differences were compared using the post hoc Bonferroni test. $P < 0.05$ was considered statistically significant.

RESULTS

Laminin-221 Enhanced Structural, Mechanical, and Metabolic Functions of hiPS-CMs

Laminin-221 selectively binds to integrin α 7 β 1,⁸ which is highly expressed in cardiomyocytes and plays a critical role in signaling, differentiation, and survival.^{1,18,19} Thus, we tested if laminin-221 could enhance structural, mechanical, and metabolic functions of hiPS-CMs. The structural function of hiPS-CMs was assessed by immunohistochemical analysis and quantitative polymerase chain reaction. Immunostaining revealed that laminin-2,

integrin α 7, and actinin were enhanced by laminin-221 (Figure 1A and 1B). The analysis of mRNA expression revealed that several genes were upregulated in hiPS-CMs cultured on laminin-221 coating plate, including genes involved in ventricular structure (*MYL2*), sarcomere structure (*TNNT3*), cardiac maturation (*MYH7*), Ca⁺ pump, and channel-related genes (*ATP2A2*, *RYR2* [ryanodine receptor 2]) (Figure 1C). As for mechanical function, contractile properties of hiPS-CMs were assessed by the Cell Motion Imaging System. Laminin-221 significantly enhanced systolic velocity (laminin versus control, 16.4±2.0 versus 11.1±3.4 μ m/s; P <0.001) and diastolic velocity (laminin versus control, 9.0±1.8 versus 6.1±2.5 μ m/s; P <0.002) of hiPS-CMs (Figure 1D). To investigate the metabolic effect of laminin-221 on hiPS-CM, we assessed the mitochondrial function of hiPS-CMs by Seahorse XF96 extracellular flux analyzer. The increase in OCR in hiPS-CMs cultured on laminin-221 coating plate suggested significant increases in oxidative metabolism. Quantitative analyses confirmed a significant increase in the maximum capacity of oxidative metabolism in laminin groups (laminin versus control, 221±30 versus 172±19 pmol/min; P <0.003) (Figure 1E). Furthermore, we evaluated the VEGF production by using ELISA. Laminin-221 enhanced

production of VEGF compared with control (laminin versus control, 1356±135 versus 937±370 pg/mL; P =0.024; Figure 1F).

Laminin-221 Improved Tolerance to Hypoxia of hiPS-CMs

Outside-in signal through integrin α 7 β 1 reduces ischemic injury of cardiomyocytes,²⁰ and tolerance to hypoxia is an important factor for cell viability and survival after transplantation of ECT.²¹ Then, we investigated laminin-221 (binds to integrin α 7 β 1 and causing outside-in signaling), on whether it enhances the tolerance to hypoxia of hiPS-CMs. To assess the tolerance to hypoxia of hiPS-CMs, we used LDH Cytotoxicity Detection Kit (Takara Bio Inc, Shiga, Japan) and Cell Counting Kit-8. After hypoxia incubation for 96 hours, LDH was released, implying that cell injury significantly decreased (cytotoxicity rate: laminin-221 versus control, 47±1% versus 51±1%; P <0.001; Figure 2A). Also, cell viability was significantly improved (survival cell counting: laminin-221 versus control, 1.27±0.5×10⁴/96 wells versus 1.13±0.5×10⁴/96 wells; P <0.001; Figure 2B) in hiPS-CMs cultured on laminin-221 coating plate (Figure 2A and 2B).

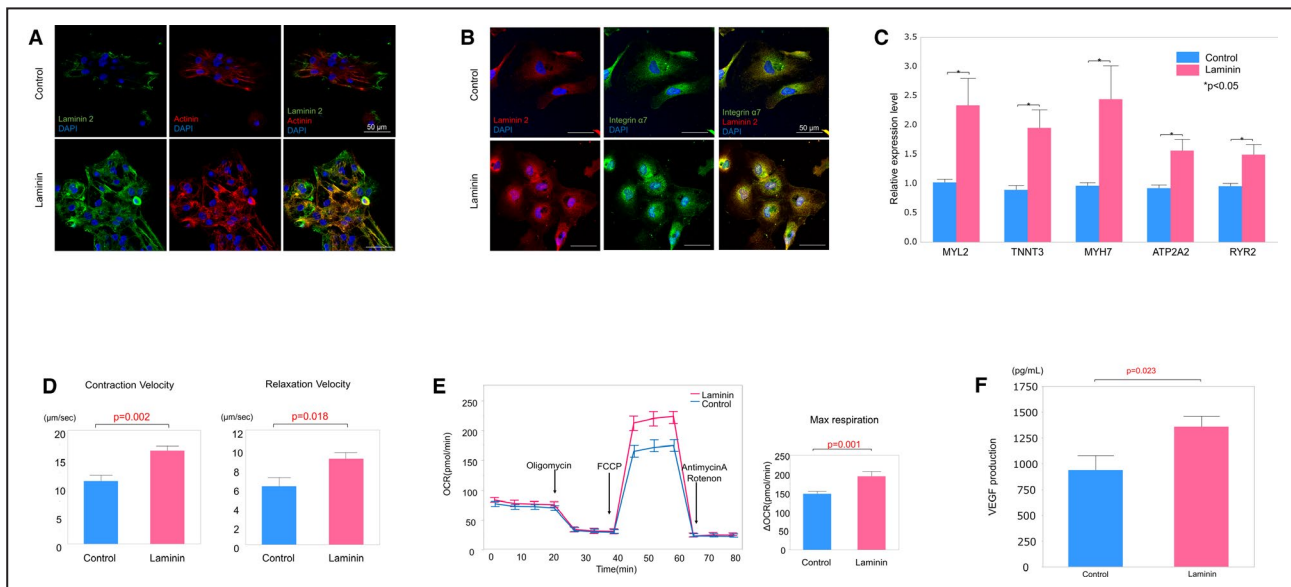


Figure 1. Laminin-221 enhanced structural, mechanical, and metabolic characterization of human-induced pluripotent stem cell-derived cardiomyocytes (hiPS-CMs).

hiPS-CMs were cultured on laminin coating dish (laminin) or not (control). **A**, Immunostaining images of actinin (red), laminin-2 (green), and nuclei (blue). **B**, Immunostaining images of laminin-2 (red), integrin α 7 (green), and nuclei (blue). Bar=50 μ m. **C**, Quantitative polymerase chain reaction analysis of gene expression in hiPS-CMs: ventricular MYL2 (myosin light chain-2), TNNT3 (troponin I), MYH7 (myosin heavy chain β), b-major histocompatibility complex, sarcoplasmic/endoplasmic reticulum calcium ATPase2 (ATPA2), and RYR2 (ryanodine receptor 2). hiPS-CMs were cultured for 4 days (n=8). **D**, Contractile property of hiPS-CMs. Left: contraction velocity. Right: relaxation velocity (n=10). **E**, Left: representative experiment shows mitochondrial respiration measured by oxygen consumption rate (OCR) in an XF24 Seahorse Flux Analyzer. Right: maximum (Max) respiration (n=10). **F**, Secretion of VEGF (vascular endothelial growth factor) (n=7). DAPI indicates 4',6-diamidino-2-phenylindole; and FCCP, carbonyl cyanide-p-trifluoromethoxyphenylhydrazone.

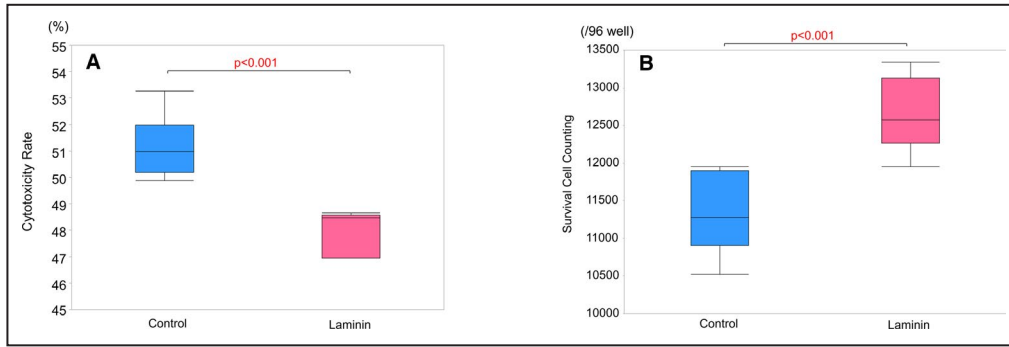


Figure 2. Laminin-221 improved tolerance to hypoxia of human-induced pluripotent stem cell-derived cardiomyocytes (hiPS-CMs).

hiPS-CMs were cultured on laminin coating dish (laminin) or not (control) under hypoxic conditions for 72 hours. **A**, Lactate dehydrogenase production (n=7). **B**, Cell viability (n=10). The horizontal line in the middle of each box indicates the median; the top and bottom borders of the box mark the 75th and 25th percentiles, respectively; and the whiskers mark the 90th and 10th percentiles.

Laminin-221 Activates FAK Signaling and Enhances Antiapoptosis-Related Gene Expression to Improve Tolerance to Hypoxia of hiPS-CMs

Next, we investigated the molecular mechanism of tolerance to hypoxia. Outside-in signaling through integrin α 7 β 1 causes FAK activation, and FAK

expression reduces apoptosis under hypoxia situation.²⁰ We investigate whether laminin-221, which binds to integrin α 7 β 1 and causes outside-in signaling, enhances FAK expression and antiapoptosis-related gene expression or not under hypoxia situation. Immunostaining and Western blotting revealed that laminin-221 enhances phosphorylated FAK (Tyr397) (Figure 3A and 3B). The analysis of mRNA expression

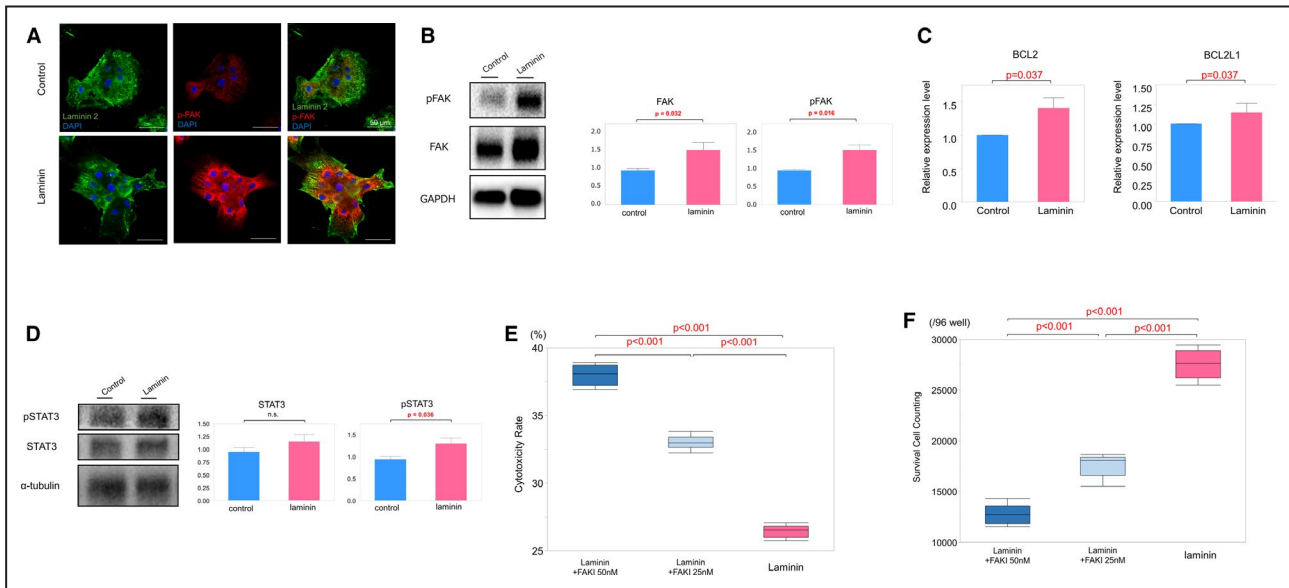


Figure 3. Laminin -221 improves tolerance to hypoxia of human-induced pluripotent stem cell-derived cardiomyocytes (hiPS-CMs).

A, Immunostaining images of phosphorylated focal adhesion kinase (FAK) (pFAK; Tyr397) (red), laminin-2 (green), and nuclei (blue). Bar=50 μ m. **B**, Western blotting analysis revealed enhancement of expression of pFAK (n=6). **C**, Quantitative polymerase chain reaction analysis of antiapoptosis-related gene expression in hiPS-CMs under hypoxic conditions: *BCL2* (B-cell leukemia/lymphoma 2) and *BCL2L1* (Bcl-2-like protein 1) (n=4). **D**, Western blotting analysis of downstream signaling related protein of FAK: *STAT3* (signal transducer and activator of transcription 3) and phosphorylated *STAT3* (pSTAT3; pS727-STAT3) (n=6). **E** and **F**, FAK inhibitor 14 causes reductions of tolerance to hypoxia of hiPS-CMs: lactate dehydrogenase production (n=7; **E**) and cell viability (n=10; **F**). The horizontal line in the middle of each box indicates the median; the top and bottom borders of the box mark the 75th and 25th percentiles, respectively; and the whiskers mark the 90th and 10th percentiles. DAPI indicates 4',6-diamidino-2-phenylindole; and n.s., not significant.

revealed that antiapoptosis-related gene (*BCL2*, *BCL2L1*) expression was significantly upregulated in hiPS-CMs cultured on laminin-221 coating plate (Figure 3C). In addition to antiapoptosis-related gene expression, STAT3 expression, which is a signaling-related protein that plays a crucial role in mitochondrial function, is essential for cell survival under hypoxic incubation.²² We investigated the effects of laminin-221 on STAT3 activation under hypoxic incubation by Western blotting. The analysis revealed that laminin-221 significantly enhanced the expression of phosphorylated STAT3, an activated form of STAT3 (Figure 3D).

Furthermore, we evaluate whether FAK inhibition reduced tolerance to hypoxia. FAK14 directly inhibits the essential Tyr397 autophosphorylation and thus subsequent total phosphorylation and activation of FAK without inhibiting other recombinant kinases. We evaluated LDH release and cell viability of hiPS-CMs incubated on the laminin-221 coating plate for 72 hours with the addition of FAK, 25 or 50 $\mu\text{mol/L}$, or no addition of FAK14 using LDH Cytotoxicity Detection Kit (Takara Bio Inc, Shiga, Japan) and Cell Counting Kit-8. LDH release and cell viability revealed that FAK14 dose dependency reduced the hypoxic tolerance of hiPS-CMs (Figure 3E and 3F).

Fabrication and Characterization of 3D-ECT of hiPS-CMs

We readily accomplished the generation of 3D-ECT using novel simple and pragmatic technique. Our technique also reproduced fabrication of arbitrary sizes (we made 1×1 cm; mega size, 2.5×2.5 cm; and giga size, 5×5 cm). The incorporation of laminin-221 to 3D-ECT, as well as proper handling of 3D-ECT, allowed for its production from diluted fibrinogen and thrombin, which enhanced the survival of hiPS-CMs. We produced 2 types of 3D-ECTs: L-ECT and ECT. L-ECT includes laminin-221, whereas ECT did not. We mixed fibrinogen, hiPS-CMs, and laminin-221 (for L-ECT) or PBS (for ECT), then dropped the mixture onto a DMEM gelatin gel, which was prepared in advance. We added thrombin, then subsequently covered the mixture by polypropylene sheet (10 × 10 mm). We solidified the 3D-ECT at 4°C for 15 minutes, then dissolved the DMEM gelatin gel under the 3D-ECT in an incubator at 37°C for 20 minutes to retrieve 3D-ECT with polypropylene sheet. Retrieving 3D-ECT with the polypropylene sheet allowed us to produce several arbitrary sizes of 3D-ECT by merely changing the size of the polypropylene sheet (Figure 4A and 4B). The 3D-ECT began to beat synchronously within 24 hours, allowing at any point for the 3D-ECT to be retrieved and transplant for cell therapy.

At first, we compared 4 different cell densities of L-ECT (1, 3, 5, and 7 million hiPS-CMs per 1 cm^2) by assessing contractile properties of 3D-ECT by the Cell

Motion Imaging System. As the cell density increased, contractile velocity increased until 5 million hiPS-CMs per 1 cm^2 . Any further increase in cell density produced a plateau in contractile velocity (Figure 4C). Then, we selected 5 million hiPS-CMs per 1 cm^2 for fabricating 3D-ECT. We also compare the impact of 10 and 20 nmol/L of laminin-221 on systolic and diastolic function of 3D-ECT, and results revealed there were no differences between the groups (Figure S1). Thus, we used 10 nmol/L of laminin-221 for 3D-ECT. Thickness of 3D-ECTs was around 150 μm (Figure 4D), and immunostaining revealed that laminin 2 and troponin T were expressed well in the 3D-ECTs (Figure 4E). The analysis of mRNA expression revealed that sarcomere structure (*TNNT3*), cardiac maturation (*MYH7*), ventricular structure (*MYL2*), and Ca^+ channel-related genes (*RYR2*) were upregulated in L-ECT compared with ECT (Figure 4F). Next, we compared L-ECT with ECT by assessing contractile properties by the Cell Motion Imaging System. L-ECTs significantly enhanced contraction velocity (L-ECT versus ECT, 14.4 ± 1.4 versus 11.3 ± 2.0 $\mu\text{m/s}$; $P=0.0049$) and relaxation velocity (L-ECT versus ECT, 6.8 ± 0.4 versus 5.4 ± 0.3 $\mu\text{m/s}$; $P=0.016$) versus ECTs (Figure 4G). Furthermore, we evaluate VEGF production by using ELISA. Laminin-221 enhanced production of VEGF (L-ECT versus ECT, 3420 ± 320 versus 2060 ± 155 pg/mL ; $P<0.001$; Figure 4H).

Three-Dimensional ECT Improves Cardiac Function and Attenuates LV Remodeling in the MI Model

For the in vivo study, we implanted L-ECT, ECT, or fibrin gel sheet on the infarct area of the heart and covered by pericardium (L-ECT group, $n=10$; ECT group, $n=10$; control group, $n=10$). To evaluate the therapeutic effects of 3D-ECT transplantation, we assessed cardiac function in MI rats using transthoracic echocardiography every week for 4 weeks after the transplantation of 3D-ECTs. Preoperative heart function, including EF, LV end-diastolic diameter, and LV end-systolic diameter, was similar in the 3 groups (EF: L-ECT versus ECT versus control, $37.5 \pm 7.2\%$ versus $37.0 \pm 8.6\%$ versus $37.8 \pm 4.7\%$, $n=10$; L-ECT versus control, $P=0.996$; L-ECT versus ECT, $P=0.985$; ECT versus control, $P=0.965$) Four weeks after transplantation, EF of L-ECT group was significantly better than the other 2 groups (L-ECT versus ECT versus control, $55.1 \pm 6.3\%$ versus $48.1 \pm 5.9\%$ versus $34.8 \pm 2.5\%$, $n=10$; L-ECT versus control, $P<0.001$; L-ECT versus ECT, $P=0.017$; ECT versus control, $P<0.001$) (Figure 5A1). In addition, improvement of EF (ΔEF : postoperative EF-preoperative EF) showed at postoperative 4 weeks that ΔEF of L-ECT group was significantly better than the other 2 groups

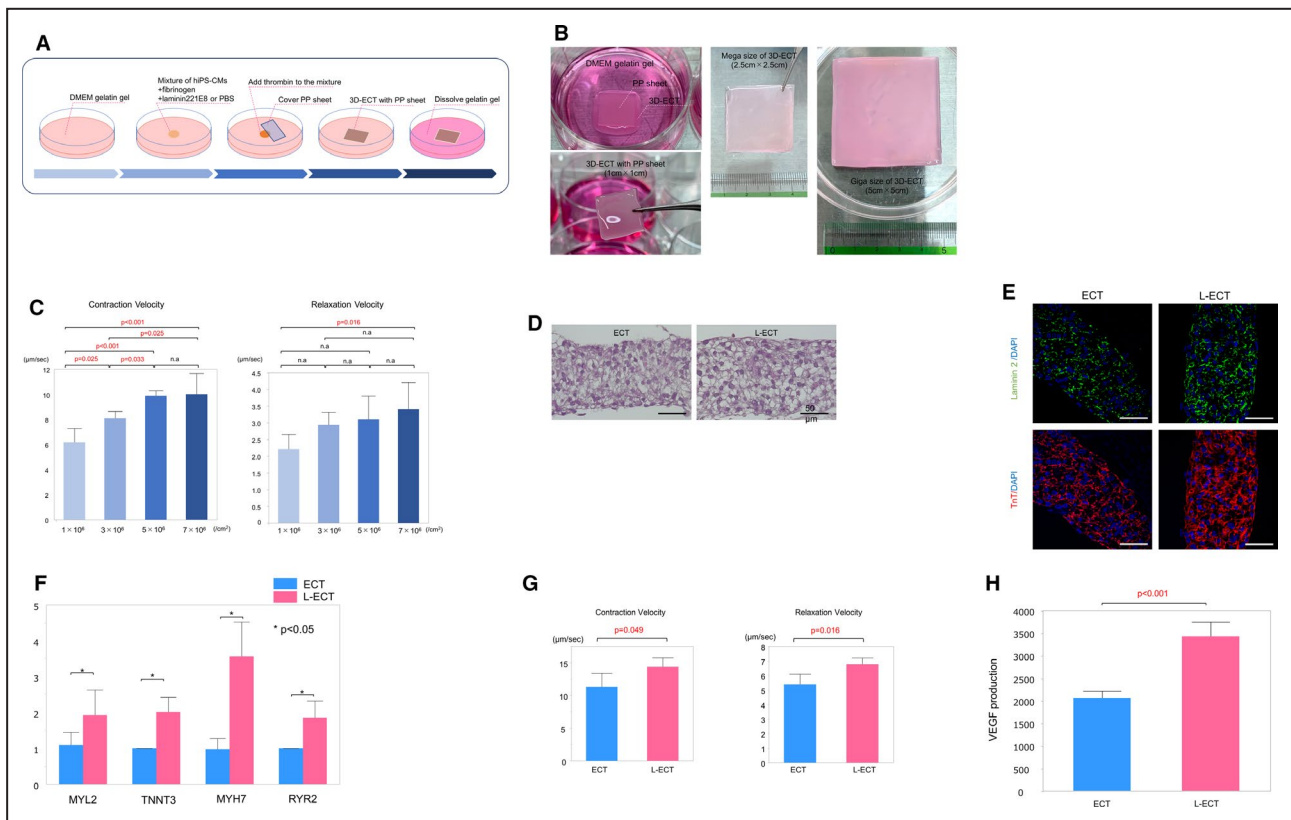


Figure 4. Fabrication and characterization of 3-dimensional engineered cardiac tissue (3D-ECT) of human-induced pluripotent stem cell-derived cardiomyocytes (hiPS-CMs).

A, Schematic representation of fabrication of 3D-ECTs. **B**, Left top: solidified the 3D-ECT on DMEM gelatin gel. Left bottom: dissolve DMEM gelatin gel to retrieve 3D-ECT with polypropylene (PP) sheet. Right: mega (2.5 × 2.5 cm) and giga (5 × 5 cm) size of 3D-ECTs. **C**, Contractile property of laminin-conjugated engineered cardiac tissue (L-ECT) with different cell density (n=4). **D**, Histology of 3D-ECTs with 5 million hiPS-CMs per 1 cm². Bar=50 µm. **E**, Immunostaining images of TnT (troponin T; red), connexin 43 (green), and nuclei (blue). Bar=50 µm. **F**, Quantitative polymerase chain reaction analysis of gene expression in 3D-ECTs: MYL2 (myosin light chain-2), TNNT3 (troponin I), MYH7 (myosin heavy chain β), and RYR2 (ryanodine receptor 2) (n=6). **G**, Contractile property of 3D-ECT. Left: contraction velocity. Right: relaxation velocity (n=4). **H**, Concentration of VEGF (vascular endothelial growth factor) (n=4). DAPI indicates 4',6-diamidino-2-phenylindole.

(L-ECT versus ECT versus control, 17.5±5.0% versus 11.1±4.2% versus -3.1±5.7%, n=10; L-ECT versus control, $P<0.001$; L-ECT versus ECT, $P=0.023$; ECT versus control, $P<0.001$) (Figure 5A2).

Furthermore, LV end-systolic diameter and LV end-diastolic diameter of L-ECT group were significantly smaller than control group (LV end-diastolic diameter: L-ECT versus ECT versus control, 7.1±0.5 versus 7.3±0.4 versus 8.2±0.3 mm, n=10; L-ECT versus control, $P<0.001$; L-ECT versus ECT, $P=0.075$; ECT versus control, $P<0.001$; LV end-systolic diameter: L-ECT versus ECT versus control, 5.3±0.5 versus 5.7±0.4 versus 7.0±0.2 mm, n=10; L-ECT versus control, $P<0.001$; L-ECT versus ECT, $P=0.016$; ECT versus control, $P<0.001$) (Figure 5B and 5C).

We assessed the cardiac structure and accumulation of interstitial fibrous components at 4 weeks after transplantation by histological analysis. Four weeks after transplantation, cell size of peri-infarct zone was significantly smaller in L-ECTs than other 2 groups

(L-ECT versus ECT versus control, 15.4±2.1 versus 19.4±2.9 versus 23.0±2.7 µm; L-ECT versus control, $P<0.001$; L-ECT versus ECT, $P<0.001$; ECT versus control, $P<0.001$) (Figure 5D). Furthermore, the ratio of fibrosis at remote zone was also significantly small in L-ECT group than in other groups (L-ECT versus ECT versus control, 3.2±0.7% versus 6.1±1.5% versus 10.0±1.0%; L-ECT versus control, $P<0.001$; L-ECT versus ECT, $P=0.003$; ECT versus control, $P<0.001$) (Figure 5E).

Three-Dimensional L-ECT Induced Angiogenesis and Angiogenic Cytokine Expression at Border Zone

Immunostaining revealed enough engraftment in the L-ECT group 4 weeks after transplantation and good angiogenesis for the L-ECT group (Figure 6A and 6B). We also assessed angiogenesis at peri-infarct zone by immunostaining. L-ECT significantly enhanced capillary

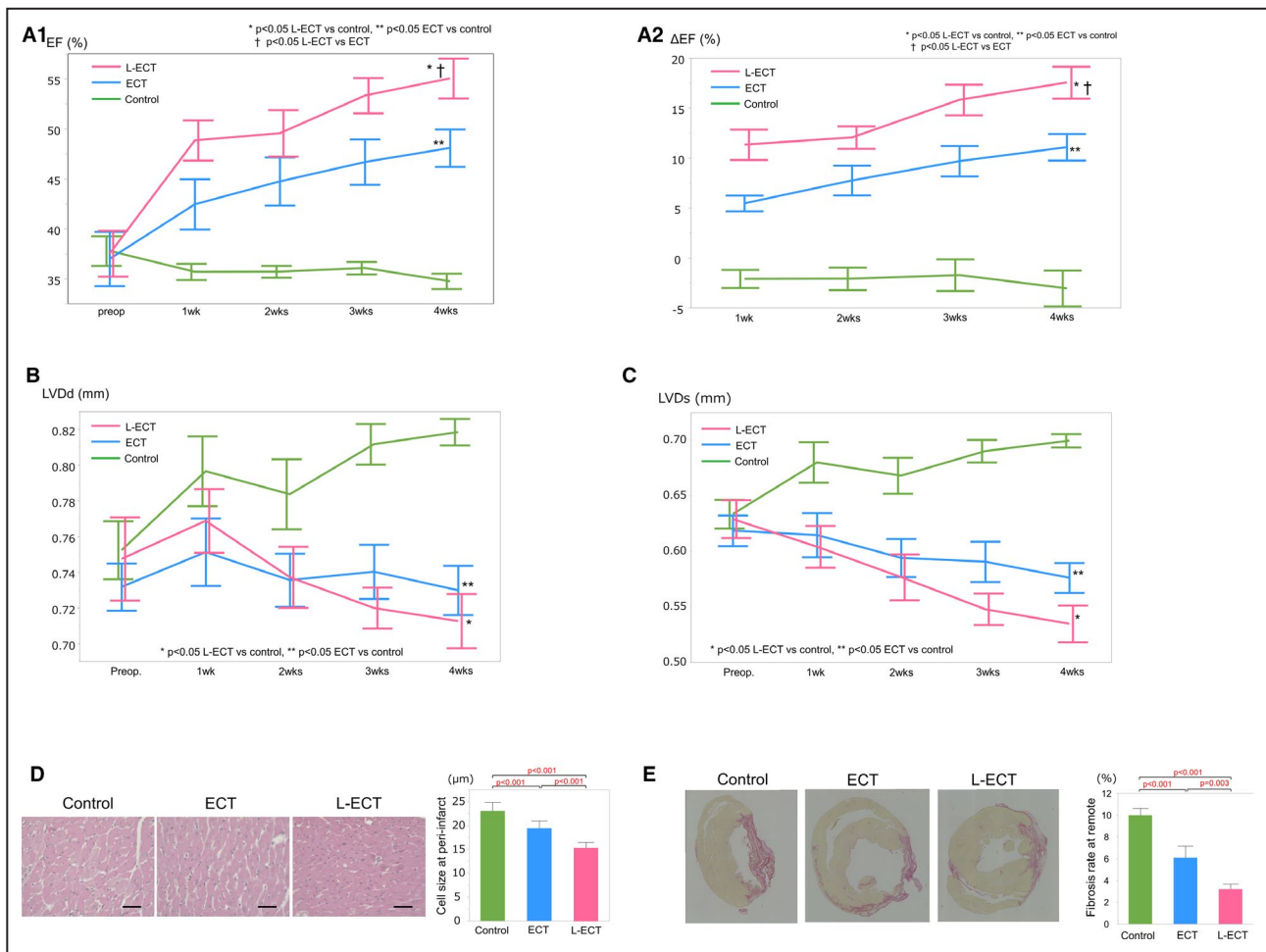


Figure 5. Laminin-conjugated engineered cardiac tissue L-ECT) improves cardiac function and attenuates left ventricular (LV) remodeling in myocardial infarction (MI) model.

A–C, Course of cardiac function in the 3 groups (L-ECT group, n=10; ECT group, n=10; control group, n=10), **A1**, LV ejection fraction (EF). **A2**, Course of improvement of EF (Δ EF). **B**, LV end-diastolic diameter (LVDd). **C**, LV end-systolic diameter (LVDs). **D**, Cell size of peri-infarct zone in MI heart 4 weeks after transplantation. Bar=50 μ m. **E**, Fibrosis rate at remote zone in MI heart 4 weeks after transplantation. Sections are assessed by Sirius Red staining. Preop indicates preoperatively.

density in the peri-infarct zone compared with the other groups (Figure 6C). Furthermore, the expression of cardioprotective and angiogenic factors in ischemic cardiomyopathic hearts at 4 weeks after treatment was evaluated by quantitative polymerase chain reaction. The relative expression levels of *VEGF*, fibroblast growth factor (*FGF*), stromal cell-derived factor 1 (*SDF-1*), and platelet-derived growth factor (*PDGF*) at the peri-infarct zone were significantly higher in the L-ECT group compared with those in the 2 other groups (Figure 6D).

L-ECT Demonstrated Good Engraftment Early on After Transplantation

Immediately after 3D-ECT implantation, tolerance to hypoxia of hiPS-CMs was crucial for engraftment, because enough microvasculature organization of transplanted 3D-ECTs is required for a few days after transplantation.²¹ Laminin-221 enhanced tolerance

to hypoxia of hiPS-CMs in vitro, and the efficacy of L-ECT occurred within a week after transplantation of 3D-ECT. We then investigated the engraftment rate of 3D-ECTs within 1 week after transplantation by using bioluminescence imaging. 3D-ECTs were made from the luciferase gene-inserted hiPS-CMs (201B7-luc7), which generated a strong bioluminescent signal before and after transplantation. Preoperative assessment of the bioluminescent signal of 3D-ECTs was relatively the same between L-ECTs and ECTs. Although the bioluminescent signal of implanted 3D-ECTs declined early on in both groups after transplantation, L-ECT hiPS-CM survival was enhanced at 3 and 7 days after transplantation (day 1: L-ECTs versus ECTs, 1351 [interquartile range: 766–2050] 10^3 versus 874 [interquartile range: 646–1240] 10^3 p/s/cm²/sr [$P=0.134$]; day 3: L-ECTs versus ECTs, 1105 [interquartile range: 641–1402] 10^3 versus 458 [interquartile range: 279–883] 10^3 p/s/cm²/sr [$P=0.046$]; day 7: L-ECTs versus ECTs, 899 [interquartile

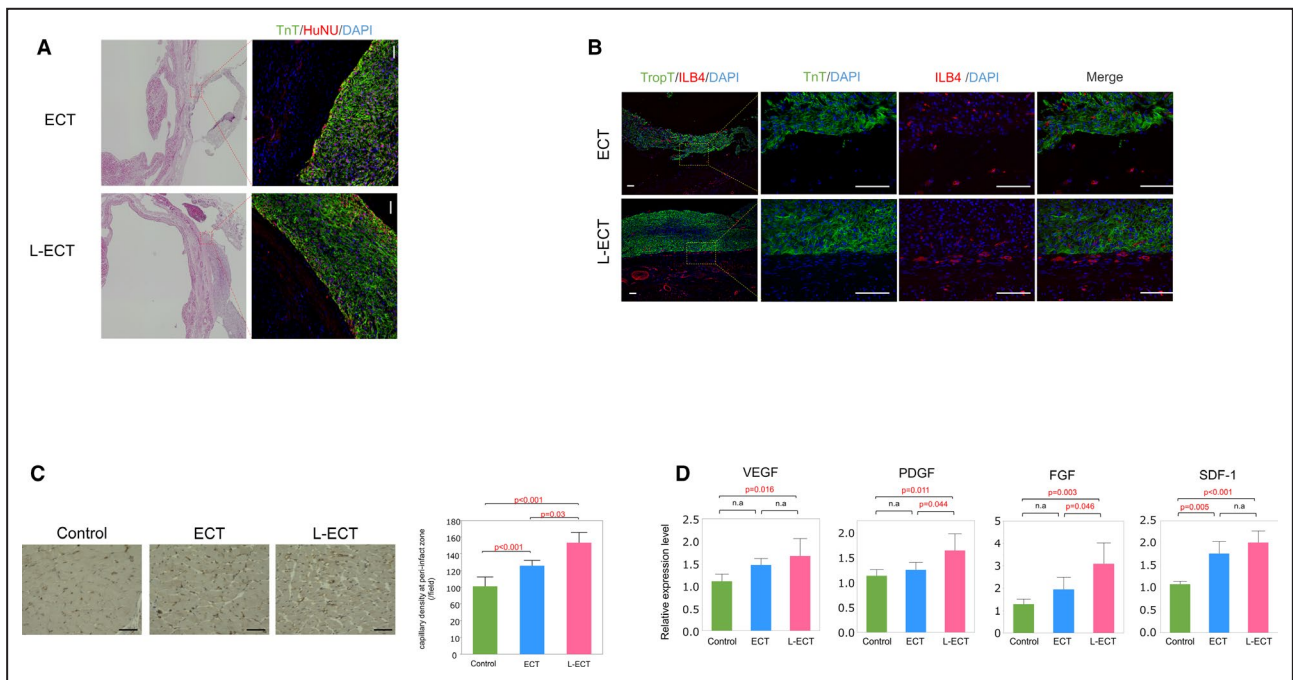


Figure 6. Laminin-conjugated engineered cardiac tissue (L-ECT) induced angiogenesis and angiogenic cytokine expression in myocardial infarction (MI) model.

A, Left: histological sections of 3-dimensional engineered cardiac tissues after being transplanted on the rat heart with MI. Right: immunostaining of human nuclei (red), TnT or Trop T (troponin T; green), and nuclei (blue). Bar=50 μ m. **B**, Immunostaining of isolectin B4 (ILB4; red), TnT (green), and nuclei (blue). Bar=50 μ m. **C**, Capillary formation at the peri-infarct zone in MI heart 4 weeks after transplantation. Sections are immunostained with von Willebrand factor. Bar=50 mm. **D**, Quantitative polymerase chain reaction analysis of angiogenic cytokine-related gene expression in peri-infarct zone: VEGF (vascular endothelial growth factor), PDGF (placental growth factor), FGF (fibroblast growth factor), and SDF-1 (stromal cell-derived factor 1) (L-ECT group, n=7; ECT group, n=7; control group, n=7). DAPI indicates 4',6-diamidino-2-phenylindole; and HuNu, human nuclear.

range: 406–1777] 10^3 versus 452 [interquartile range: 169–699] 10^3 p/s/cm²/sr [$P=0.093$] (Figure 7A and 7B).

Three-Dimensional ECT Synchronized Pulsatile on Rat Hearts 3 Weeks After Transplantation and Has the Possibility of Direct Effect

Finally, in the present study, we investigated the possibility of a synchronized beating effect of 3D-ECT by

assessing the electrical coupling of transplanted 3D-ECT and rat heart using in vivo imaging. We monitored recipient heart and 3D-ECT, which contains gCaMP3, with high spatial and temporal resolution. Three weeks after transplantation, we performed a second thoracotomy and reopened the pericardium under 3% to 4% inhaled isoflurane anesthesia. In vivo imaging using gCaMP3 revealed spontaneous beating of 3D-ECT on the recipient rat heart (Figure 8A, Video S1). There were 4 times of rat heart beating for every 1 3D-ECT

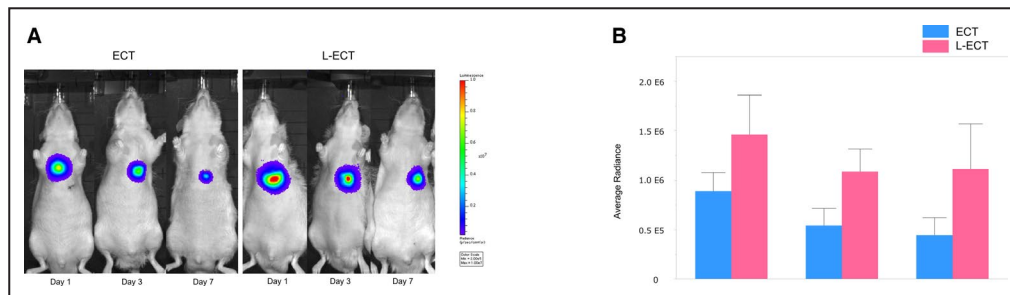


Figure 7. Laminin-conjugated engineered cardiac tissue (L-ECT) shows functional engraftment early on after transplantation.

A, Representative bioluminescence images of a single L-ECT and ECT after transplantation. **B**, Laminin improves 3-dimensional ECT graft survival early after transplantation (n=6).

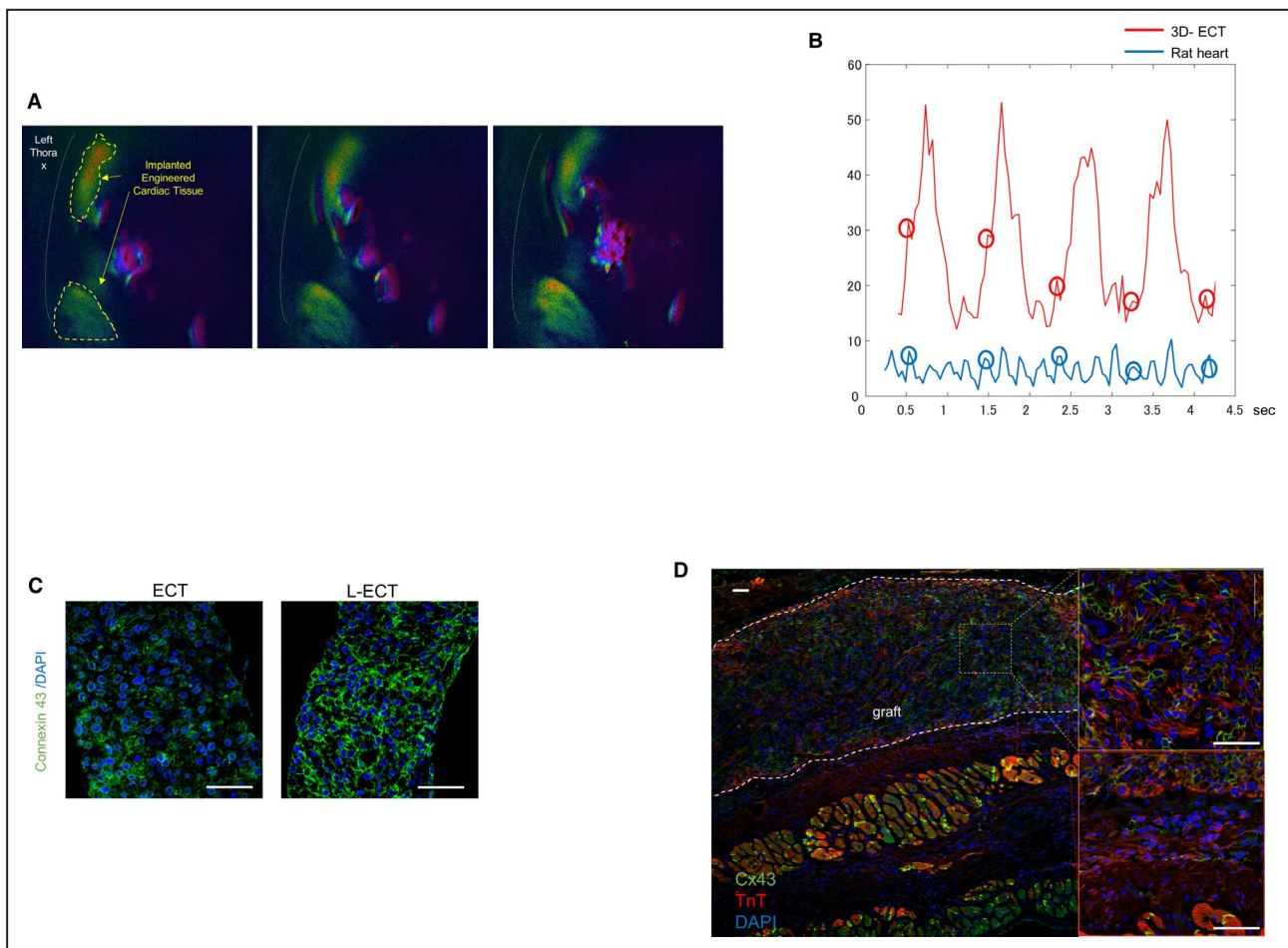


Figure 8. In vivo imaging of 3-dimensional engineered cardiac tissues (3D-ECTs).

A, Representative image of laminin-conjugated ECT 3 weeks following implantation: gCaMP6 (green). **B**, Beating rate of 3D-ECT (red) and rat heart (blue). **C**, Immunostaining of TnT (troponin T; red), connexin 43 (Cx43; green), and nuclei (blue) for 3D-ECT. Bar=50 μ m. **D**, Immunostaining of TnT (red), Cx43 (green), and nuclei (blue) in vivo. Bar=50 μ m. DAPI indicates 4',6-diamidino-2-phenylindole.

beating (Figure 8B). We also assessed the electrical coupling by alignment of connexin 43 in 3D-ECT and rat heart using immunostaining. Immunostaining assessment revealed good expression of connexin 43 in 3D-ECT in vitro and in vivo (Figure 8C and 8D).

DISCUSSION

The present study demonstrated the following points: (1) Laminin-221 enhances the functional metrics of hiPS-CMs, including mechanical and metabolic functions, and the secretion of VEGF, by activation of outside-in signaling via integrin. (2) Laminin-221 enhances survival of hiPS-CMs under hypoxic conditions by upregulation of antiapoptotic-related gene expression through in vitro FAK activation. (3) A simple and pragmatic technique to fabricate 3D-ECT conjugated with laminin-221 was established, and the presence of laminin-221 enhances the mechanical function and

VEGF secretion of 3D-ECT. (4) Laminin-221 enhanced engraftment of 3D-ECT in vivo transplantation with improvement in the cardiac function in a rat model of MI. (5) Transplanted 3D-ECT conjugated with laminin-221 achieved synchronized contraction with the recipient heart 3 weeks after transplantation.

Binding to specific ECM and activation of outside-in signaling are crucial for many types of cells to survive. Furthermore, the detachment of specific ECM and cells results in a type of apoptosis known as anoikis.^{10,12} The binding between cells and cell-specific ECM forming a niche is also important for the organization, maturation, and maintenance of tissues. Specifically, the absence of hiPS-CM-specific ECM might result in poor niche establishment and reduce the viability of hiPS-CMs, which, in turn, may decrease therapeutic efficiency.^{4,23} This relationship can be easily connected with practical application of ECM modulation for myocardial tissue engineering.

Laminin is one of the components of the ECM and has 16 different isoforms. Laminin-221 is a subtype of laminin and selectively binds to integrin $\alpha 7 \beta 1$, which is expressed on the surface of hiPS-CMs.^{8,9,16} Laminin-221 plays a crucial role in the enhancement of differentiation, growth, and viability of hiPS-CMs through outside-in signaling. In addition, detachment of integrin from laminin causes anoikis of hiPS-CMs.^{8,10} hiPS-CM transplantation has been previously performed and revealed therapeutic efficacy. However, because of poor engraftment or performance of transplanted cardiac tissue, this effect is not dependent on cardiomyogenesis, and instead results mainly from cytokine paracrine effects. Therefore, there remains a need to bring out the maximum characteristics of cardiac tissue with the capability to directly restore mechanical force to the distressed myocardium.^{4,6} To this end, we recently revealed that transplantation of engineered tissue with hiPS-CMs achieved electrical synchronization with the native heart, implying that transplanted hiPS-CMs have the potential to provide a direct effect to failed heart.^{24,25} Thus, enhancement of structural function and viability of transplanted hiPS-CMs by addition of hiPS-CM-specific ECM may enhance therapeutic efficacy and potential, including paracrine effects and synchronized beating of transplanted hiPS-CMs.

In our *in vitro* study, laminin-221 was found to enhance the mechanical and metabolic functions of hiPS-CMs. As for mechanical function, a previous study demonstrated that matured hiPS-CMs enhance systolic and diastolic function.²⁶ In addition, activation of integrin interacts with RYR2, a calcium release channel, to control the mechanical function of cardiomyocytes.¹⁸ In the present study, ATP2A2, a calcium uptake channel, and RYR2 gene expression were upregulated by laminin-221. We estimated that the binding of laminin-221 and integrin resulted in outside-in signaling that upregulates ATP2A2 and RYR2 gene expression and may enhance systolic and diastolic function of hiPS-CMs. As for metabolic function, laminin-221 enhanced the maximum respiration speed of hiPS-CMs. A previous study demonstrated that outside-in signaling through integrins causes downstream activation of FAK and STAT3, ultimately enhancing mitochondrial function.²² Our results also found upregulation of activated FAK and STAT3, implying that binding of laminin and integrin enhances mitochondrial function through the activation of FAK and STAT3. Furthermore, laminin-221 improves tolerance to hypoxia, as evidenced by reduced LDH production and improved viability of hiPS-CMs after incubation in hypoxic conditions. We also observed that binding of laminin-221 and integrin $\alpha 7 \beta 1$ causes FAK activation and enhances antiapoptosis-related

gene expression (*BCL1* and *BCL2L1*), resulting in prevention of hypoxia-induced apoptosis. These changes in intercellular signaling in cardiomyocytes by additional laminins may support the mechanisms of enhanced mechanical and metabolic function of hiPS-CMs (Figure S2).

In an *in vivo* study, 4 weeks after transplantation, we found good engraftment of L-ECT with improved cardiac function. Laminin-221 enhanced expression of angiogenic factors, especially for VEGF, as paracrine effect to increase capillary density significantly and reduction in hypertrophy and fibrosis. These results imply that, in the L-ECT group, LV remodeling was reduced because of enhancement of paracrine effects, supported by good engraftment and enhancement of secreting angiogenic factors. A previous study reported that, immediately after 3D-ECT implantation, tolerance to hypoxia of hiPS-CMs was crucial for engraftment because of the microvasculature organization of transplanted 3D-ECTs occurring in the few days immediately after transplantation.²¹ *In vivo* studies have revealed good engraftment of L-ECT even under hypoxic conditions, which may depend on the tolerance to hypoxia of hiPS-CMs attributable to adjuvant laminin in the *in vivo* transplant. In clinical scenario, conjugating of laminin-221 to hiPS-CMs has the potential not only to improve therapeutic efficacy but also to reduce transplanted number of hiPS-CMs, which has the advantage in reduction of cost and complication of hiPS-CM transplantation.

There were a few limitations to this study. Although we mainly focused on relationship of laminin-221 and hiPS-CM viability, immune response to the graft, including immune suppression of macrophage, also has the potential to relate to therapeutic efficacy; we did not assess enough for these factors. We need further study to reveal relationship of ECM and immune response. However, our study provides novel information on laminin substrate for tissue engineering of the heart.

Laminin-221 enhanced mechanical and metabolic functions of hiPS-CMs *in vitro*, and demonstrated improved therapeutic potential of 3D-ECT in a rat ischemic cardiomyopathy model, suggesting that adjuvant laminin-221 may increase the clinical benefit of hiPS cell-derived cardiac constructs.

ARTICLE INFORMATION

Received January 7, 2020; accepted May 15, 2020.

Affiliations

From the Department of Cardiovascular Surgery, Osaka University Graduate School of Medicine (T.S., S.M., T.K., S.F., J.Y., M.T., A.H., F.O., K.T., Y.S.), Division of Matrixome Research and Application, Institute for Protein Research, Osaka University (R.S.-N., K.S.); and Department of Immunology and Regenerative Medicine, Osaka University Graduate School of Medicine, Osaka, Japan (T.T.).

Acknowledgments

We thank Seiko Eiraku for technical support.

Sources of Funding

This work was supported by Japan Society for the Promotion of Science KAKENHI grant JP18K16389.

Disclosures

None.

Supplementary Materials

Tables S1–S2

Figures S1–S2

Video S1

REFERENCES

- Cohn JN. Heart failure in 2013: continue what we are doing to treat HF, but do it better. *Nat Rev Cardiol*. 2014;11:69–70.
- Longnus SL, Mathys V, Dornbierer M, Dick F, Carrel TP, Tevearai HT. Heart transplantation with donation after circulatory determination of death. *Nat Rev Cardiol*. 2014;11:354–363.
- Abraham WT, Smith SA. Devices in the management of advanced, chronic heart failure. *Nat Rev Cardiol*. 2013;10:98–110.
- Kawamura M, Miyagawa S, Miki K, Saito A, Fukushima S, Higuchi T, Kawamura T, Kuratani T, Okano T, Sawa Y, et al. Feasibility, safety, and therapeutic efficacy of human induced pluripotent stem cell-derived cardiomyocyte sheets in a porcine ischemic cardiomyopathy model. *Circulation*. 2012;126:S29–S37.
- Li J, Minami I, Shiozaki M, Yu L, Yajima S, Miyagawa S, Shiba Y, Morone N, Fukushima S, Sawa Y, et al. Human pluripotent stem cell-derived cardiac tissue-like constructs for repairing the infarcted myocardium. *Stem Cell Rep*. 2017;9:1546–1559.
- Miyagawa S, Fukushima S, Imanishi Y, Kawamura T, Mochizuki-Oda N, Masuda S, Sawa Y. Building a new treatment for heart failure-transplantation of induced pluripotent stem cell-derived cells into the heart. *Curr Gene Ther*. 2016;16:5–13.
- Kainuma S, Mitsuno M, Toda K, Funatsu T, Nakamura T, Miyagawa S, Yoshikawa Y, Fukushima S, Yoshioka D, Sawa Y, et al. Dilated left atrium as a predictor of late outcome after pulmonary vein isolation concomitant with aortic valve replacement and/or coronary artery bypass grafting. *Eur J Cardiothorac Surg*. 2015;48:765–777; discussion 777.
- Nishiuchi R, Takagi J, Hayashi M, Ido H, Yagi Y, Sanzen N, Tsuji T, Yamada M, Sekiguchi K. Ligand-binding specificities of laminin-binding integrins: a comprehensive survey of laminin-integrin interactions using recombinant alpha3beta1, alpha6beta1, alpha7beta1 and alpha6beta4 integrins. *Matrix Biol*. 2006;25:189–197.
- Sato-Nishiuchi R, Li S, Ebisu F, Sekiguchi K. Recombinant laminin fragments endowed with collagen-binding activity: a tool for conferring laminin-like cell-adhesive activity to collagen matrices. *Matrix Biol*. 2018;65:75–90.
- Miyagawa S, Sawa Y, Taketani S, Kawaguchi N, Nakamura T, Matsuura N, Matsuda H. Myocardial regeneration therapy for heart failure: hepatocyte growth factor enhances the effect of cellular cardiomyoplasty. *Circulation*. 2002;105:2556–2561.
- Takeda M, Miyagawa S, Fukushima S, Saito A, Ito E, Harada A, Matsuura R, Iseoka H, Akashi M, Sawa Y, et al. Development of in vitro drug-induced cardiotoxicity assay by using three-dimensional cardiac tissues derived from human induced pluripotent stem cells. *Tissue Eng Part C Methods*. 2018;24:56–67.
- Sougawa N, Miyagawa S, Fukushima S, Yokoyama J, Kitahara M, Harada A, Mochizuki-Oda N, Sato-Nishiuchi R, Sekiguchi K, Sawa Y. Laminin-511 supplementation enhances stem cell localization with suppression in the decline of cardiac function in acute infarct rats. *Transplantation*. 2019;103:e119–e127.
- Matsuura K, Wada M, Shimizu T, Haraguchi Y, Sato F, Sugiyama K, Konishi K, Shiba Y, Ichikawa H, Okano T, et al. Creation of human cardiac cell sheets using pluripotent stem cells. *Biochem Biophys Res Commun*. 2012;425:321–327.
- Burridge PW, Matsa E, Shukla P, Lin ZC, Churko JM, Ebert AD, Lan F, Diecke S, Huber B, Mordwinkin NM, et al. Chemically defined generation of human cardiomyocytes. *Nat Methods*. 2014;11:855–860.
- Taniguchi Y, Ido H, Sanzen N, Hayashi M, Sato-Nishiuchi R, Futaki S, Sekiguchi K. The C-terminal region of laminin beta chains modulates the integrin binding affinities of laminins. *J Biol Chem*. 2009;284:7820–7831.
- Sekiguchi K, Hakomori S. Domain structure of human plasma fibronectin: differences and similarities between human and hamster fibronectins. *J Biol Chem*. 1983;258:3967–3973.
- Shadrin IY, Allen BW, Qian Y, Jackman CP, Carlson AL, Juhas ME, Bursac N. Cardiopatch platform enables maturation and scale-up of human pluripotent stem cell-derived engineered heart tissues. *Nat Commun*. 2017;8:1825.
- Israeli-Rosenberg S, Manso AM, Okada H, Ross RS. Integrins and integrin-associated proteins in the cardiac myocyte. *Circ Res*. 2014;114:572–586.
- Yu T, Miyagawa S, Miki K, Saito A, Fukushima S, Higuchi T, Kawamura M, Kawamura T, Ito E, Sawa Y, et al. In vivo differentiation of induced pluripotent stem cell-derived cardiomyocytes. *Circ J*. 2013;77:1297–1306.
- Cheng Z, DiMichele LA, Hakim ZS, Rojas M, Mack CP, Taylor JM. Targeted focal adhesion kinase activation in cardiomyocytes protects the heart from ischemia/reperfusion injury. *Arterioscler Thromb Vasc Biol*. 2012;32:924–933.
- Shimizu T, Sekine H, Isoi Y, Yamato M, Kikuchi A, Okano T. Long-term survival and growth of pulsatile myocardial tissue grafts engineered by the layering of cardiomyocyte sheets. *Tissue Eng*. 2006;12:499–507.
- Visavadiya NP, Keasey MP, Razskazovskiy V, Banerjee K, Jia C, Lovins C, Wright GL, Hagg T. Integrin-FAK signaling rapidly and potently promotes mitochondrial function through STAT3. *Cell Commun Signal*. 2016;14:32.
- Masumoto H, Nakane T, Tinney JP, Yuan F, Ye F, Kowalski WJ, Minakata K, Sakata R, Yamashita JK, Keller BB. The myocardial regenerative potential of three-dimensional engineered cardiac tissues composed of multiple human iPS cell-derived cardiovascular cell lineages. *Sci Rep*. 2016;6:29933.
- Iseoka H, Miyagawa S, Fukushima S, Saito A, Masuda S, Yajima S, Ito E, Sougawa N, Takeda M, Sawa Y, et al. Pivotal role of non-cardiomyocytes in electromechanical and therapeutic potential of induced pluripotent stem cell-derived engineered cardiac tissue. *Tissue Eng Part A*. 2018;24:287–300.
- Higuchi T, Miyagawa S, Pearson JT, Fukushima S, Saito A, Tsuchimochi H, Sonobe T, Fujii Y, Yagi N, Sawa Y, et al. Functional and electrical integration of induced pluripotent stem cell-derived cardiomyocytes in a myocardial infarction rat heart. *Cell Transplant*. 2015;24:2479–2489.
- Yang X, Pabon L, Murry CE. Engineering adolescence: maturation of human pluripotent stem cell-derived cardiomyocytes. *Circ Res*. 2014;114:511–523.

Supplemental Material

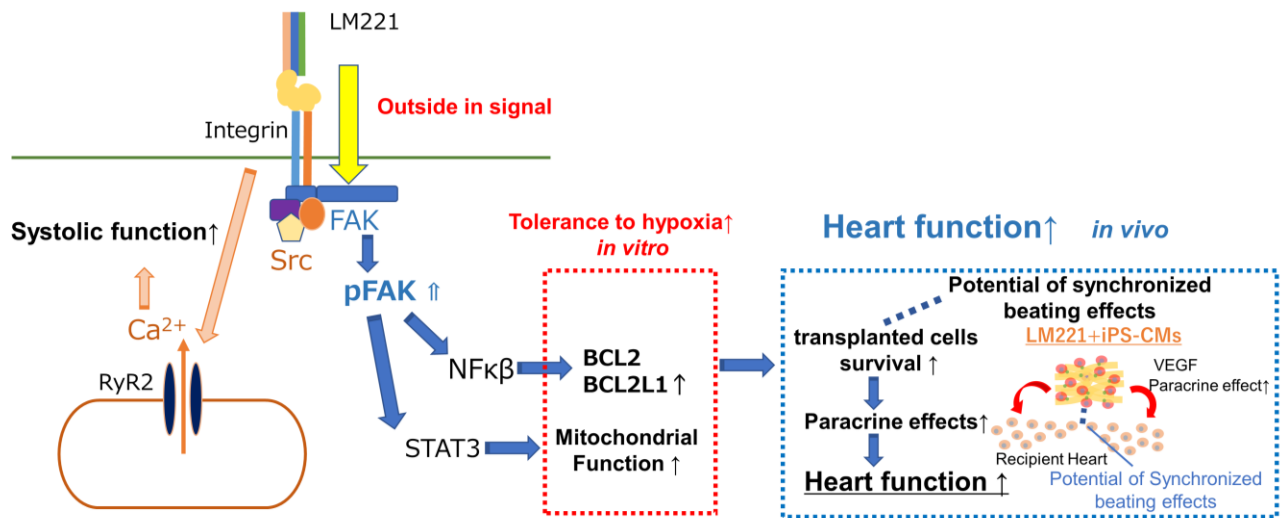
Table S1. Lists of Primers.

Gene Name	Primer
MYL2	TaqMan Hs00166405_m1
TNNT3	TaqMan Hs00943911_m1
MYH7	TaqMan Hs01110632_m1
ATPA2	TaqMan Hs00544877_m1
RYR2	TaqMan Hs00181461_m1
BCL2	TaqMan Hs00608023_m1
BCL2L1	TaqMan Hs00236329_m1
GAPDH	TaqMan Hs99999905_m1
Vegfa	TaqMan Rn01511601_m1
Pdgfb	TaqMan Rn01502596_m1
Fgf2	TaqMan Rn00570809_m1
Cxcl12	TaqMan Rn00573260_m1
GAPDH	TaqMan Rn01775763_g1

Table S2. Lists of Primary and Secondary Antibodies.

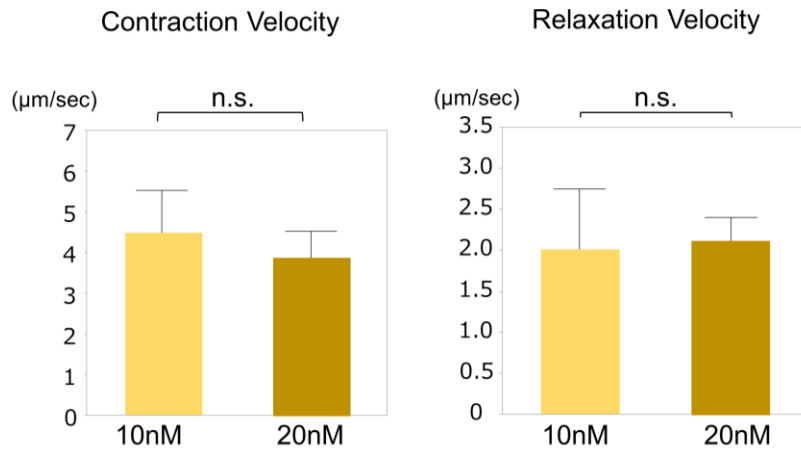
Antibody	Source
Laminin-2 α	abcom, ab11576
Sarcomeric Alpha Actinin	abcom, ab9465
Integrin α 7	Sigma, HPA008427
pFAK	abcom, ab81298
Troponin T	abcom, ab45932
HuNU	chemicon, MAB1281
Connexin43	Sigma, C6219
vWF	Millipore, MABT856
Hoechst33342	Dojindo, H342
Isolectin GS-IB4, Alexa Fluor568	Thermo Fisher scientific, I21412
Alexa fluor 488 goat anti mouse IgG	Thermo Fisher scientific, A21042
Alexa fluor 488 goat anti rabbit IgG	Thermo Fisher scientific, A11034
Alexa fluor 488 goat anti rat IgG	Thermo Fisher scientific, A11006
Alexa fluor 555 goat anti mouse IgG	Thermo Fisher scientific, A21424
Alexa fluor 555 goat anti rabbit IgG	Thermo Fisher scientific, A21429
Alexa fluor 555 goat anti rat IgG	Thermo Fisher scientific, A21434

Figure S1. Comparison of 10nM and 20nM of laminin221 on systolic and diastolic function of 3D-ECT.



Left: contraction velocity, Right: relaxation velocity, (n = 4)

Figure S2. Outside-in Signaling of Laminin-221 and Integrin $\alpha7\beta1$.



Video Legend:

Video S1. 3D-ECT was beating spontaneously before transplantation and In vivo imaging revealed that synchronized beating of 3D-ECT (left lower part) with the recipient rat heart. There were four times of rat heart beating for every one 3D-ECT beating. Best viewed with Windows Media Player.